

# Variations in the broadband spectra of BL Lac objects: millimetre observations of an X-ray-selected sample

J. A. Stevens<sup>\*</sup> and W. K. Gear<sup>\*</sup>

*Mullard Space Science Laboratory, University College London, Holmbury St. Mary, Dorking, Surrey, RH5 6NT*

draft 1.0

## ABSTRACT

Observations at millimetre wavelengths are presented for a representative sample of 22 X-ray-selected BL Lac objects (XBLs). This sample comprises 19 High-energy cutoff BL Lac objects (HBLs), 1 Low-energy cutoff BL Lac object (LBL) and 2 ‘intermediate’ sources. Data for LBLs, which are mostly radio selected BL Lac objects (RBLs) are taken from the literature. It is shown that the radio–millimetre spectral indices of HBLs ( $\bar{\alpha}_{5-230} = -0.29 \pm 0.15$ ) are slightly steeper than those of the LBLs ( $\bar{\alpha}_{5-230} = -0.19 \pm 0.14$ ). A correlation exists between  $\alpha_{5-230}$  and 230 GHz luminosity. While this correlation could be an artefact of comparing two populations of BL Lac objects with intrinsically different radio properties it is also consistent with the predictions of existing unified schemes which relate BL Lac objects to Fanaroff-Riley class I radio galaxies.

The HBLs have significantly flatter submillimetre–X-ray spectral indices ( $\bar{\alpha}_{230-X} = -0.68 \pm 0.07$ ) than the LBLs ( $\bar{\alpha}_{230-X} = -1.08 \pm 0.06$ ) although the two intermediate sources also have intermediate values of  $\alpha_{230-X} \sim -0.9$ . It is argued that this difference cannot be explained entirely by the viewing angle hypothesis and requires a difference in physical source parameters. The  $\alpha_{230-X}$  values for the HBLs are close to the canonical value found for large samples of radio sources and thus suggest that synchrotron radiation is the mechanism that produces the X-ray emission. As suggested by Padovani & Giommi, the inverse-Compton mechanism is likely to dominate in the LBLs requiring the synchrotron spectra of these sources to steepen or cutoff at lower frequencies than those of the HBLs.

**Key words:** galaxies: active – BL Lacertae objects: general – radiation mechanisms: non-thermal – radio continuum: galaxies

## 1 INTRODUCTION

More BL Lac objects have now been discovered with X-ray surveys than with radio surveys. By definition, objects selected by the two techniques share many common properties such as compact core-jet structures, lack of or weak emission lines, rapid and large amplitude optical and radio variability, high and variable linear polarization and flat radio spectra. These general properties are universally attributed to the presence of a relativistic jet that is inclined towards the line-of-sight (e.g. Blandford & Rees 1978).

There are, however, several differences between XBLs and RBLs. Most strikingly, XBLs have significantly lower apparent radio luminosities than RBLs (e.g. Stocke et al. 1990) whilst both classes have similar apparent X-ray luminosities (Sambruna et al. 1994 and references therein). Additionally, XBLs typically have lower optical polarizations

and optical variability amplitudes (Schwartz et al. 1989; Jannuzi, Green & French 1993a; Jannuzi, Smith & Elston 1993b), different parsec-scale radio properties (Kollgaard et al. 1996a), may exhibit negative evolution (Morris et al. 1991; Perlman et al. 1996a; Bade et al. 1998) while RBLs exhibit positive evolution (Stickel et al. 1991) and have a larger galaxy fraction in their optical images (Wurtz 1994) and near-infrared colours (Gear 1993a). Furthermore, XBLs may exhibit steeper X-ray spectra than RBLs but this result is only strictly true when comparing high-energy cutoff BL Lac objects (HBLs) which are mostly XBLs with low-energy cutoff BL Lac objects (LBLs) which are mostly RBLs (Padovani & Giommi 1996; Urry et al. 1996; see also Section 2).

Two competing models have been devised that attempt to explain at least some of these differences: (1) the beaming model in which XBLs are seen at larger angles to the line-of-sight than are RBLs (e.g. Ghisellini & Maraschi 1989; Padovani & Urry 1991; Ghisellini et al. 1993) and (2) a

<sup>\*</sup> E-mail: jas@mssl.ucl.ac.uk(JAS); wkpg@mssl.ucl.ac.uk(WKG)

model in which the cutoff frequency due to synchrotron radiative losses is at higher frequencies for XBLs (UV–X-ray) than for RBLs (optical–IR; Padovani & Giommi 1996 and references therein).

For the latter model, the difference in radio power between the two classes can be explained as a selection effect whereas the beaming model accounts for this difference in a natural way, although the jets have to accelerate between the X-ray emitting region and the radio emitting region in order to reproduce the observed behaviour.

Recent studies suggest that the beaming model in combination with an intrinsic spread of physical jet properties may provide the best match to the available data (Sambruna, Maraschi & Urry 1996; Georganopoulos & Marscher 1998; Fossati et al. 1998).

This paper presents new millimetre wavelength observations of a representative sample of 22 XBLs. A previous study that included data in this band (Gear 1993b) hinted that XBLs and RBLs exhibit similar radio–millimetre spectral indices but different millimetre–X-ray spectral indices, indicating that any differences between the two classes will be more apparent in the X-ray band. These results were based on a very small number of sources, however, and so the aim of this study is to provide a similar analysis for a larger number of objects. Throughout this paper we assume the Hubble constant,  $H_0 = 50 \text{ Kms}^{-1}\text{Mpc}^{-1}$ ,  $\Omega_0 = 0$  and spectral indices are written as  $S_\nu \propto \nu^\alpha$ .

## 2 SAMPLE

BL Lac objects occupy a distinct region of the  $\alpha_{ox} - \alpha_{ro}$  plane (Stocke et al. 1990). In fact, it was initially found that the RBLs and XBLs occupied two distinct regions but as more XBLs were discovered the separation became less pronounced (see below). The distribution is shown in Fig. 1 which includes RBLs from the ‘1 Jansky’ sample (Stickel et al. 1991) and XBLs predominantly from the *Einstein* Medium Sensitivity Survey (EMSS; e.g. Perlman et al. 1996a), the *Einstein* Slew Survey (Perlman et al. 1996b) and the *ROSAT* all-sky survey (Kock et al. 1996; Nass et al. 1996; Bade et al. 1998). Also included are sources from the Deep X-ray Radio Blazar Survey (DXRBS) which were found by correlating the *ROSAT* WGACAT database with several radio surveys (Perlman et al. 1998). Some BL Lac objects discovered in the *ROSAT* surveys tend to populate the  $\alpha_{ox} - \alpha_{ro}$  plane in the region between the ‘1 Jansky’ RBLs and the *Einstein* XBLs and can be considered intermediate objects. Note also that many of the DXRBS sources have colours typical of the RBLs.

We selected predominantly those sources with 4.85 GHz fluxes greater than 50 mJy but included fainter sources in an attempt to populate the  $\alpha_{ox} - \alpha_{ro}$  plane in a uniform manner. Those sources with detections at millimetre wavelengths are shown as filled symbols in Fig. 1; millimetre XBL observations are either from this study (see Table 1) or from Gear (1993b) whilst the millimetre RBL observations are from Gear et al. (1994).

Two of the sources, 1ES 0446+449 and 1ES 0715–4259, have radio structures typical of radio galaxies (Perlman et al. 1996b) and are not considered as XBLs in the following analysis. Furthermore, it has been pointed out by Giommi

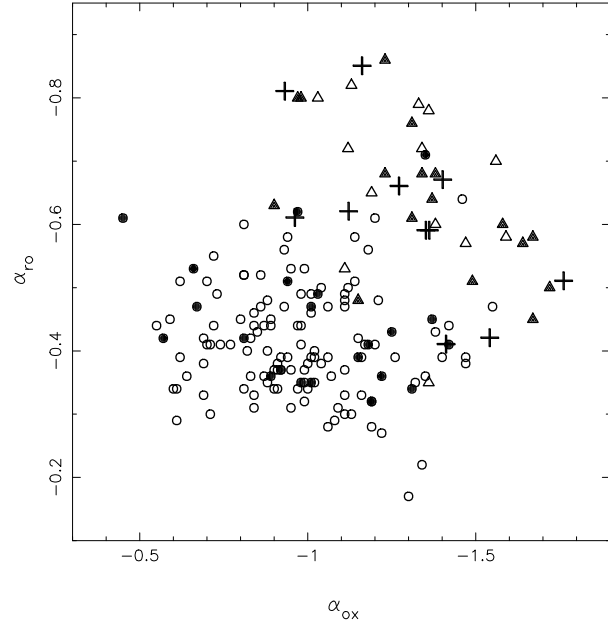


**Figure 1.** The distribution of BL Lac objects on the  $\alpha_{ox} - \alpha_{ro}$  plane. XBLs are represented by circles and ‘1 Jansky’ RBLs are represented by triangles. Those sources highlighted with filled symbols have detections at 1.35 mm ( $\sim 230$  GHz). For completeness, new BL Lac objects from the DXRBS survey (see text) are shown as crosses; millimetre observations were not made for any of these sources.

& Padovani (1994) and Padovani & Giommi (1995a) that the XBL/RBL distinction is not based on physical parameters but only on the selection band and indeed several BL Lac objects are common to both samples. These authors proposed that BL Lac objects can be split into HBLs and LBLs based on the ratio of X-ray to radio flux density ( $f_x/f_r$ ). More recent results point to a continuous range of peak frequencies, making the HBL/LBL distinction itself obsolete (e.g. Padovani 1999) but since this paper is largely concerned with a comparison of BL Lac objects selected from the two ends of the radio luminosity function the HBL/LBL approach is also considered here. The ratio  $\log(f_x/f_r)$  (X-ray fluxes measured at 1 KeV and radio fluxes at 5 GHz; both quantities in Jy) is calculated for both the ‘1 Jansky’ sample and for the objects observed in Table 1. The LBL sample is defined as comprising those objects with  $\log(f_x/f_r) < -6.25$ , the HBL sample has  $\log(f_x/f_r) > -5.75$  and an ‘intermediate’ sample, defined by  $-6.25 < \log(f_x/f_r) < -5.75$  contains only two sources, namely RXJ 12302+2512 and EXO 1811.7+3143.

It turns out that, apart from the two intermediate sources, all of the XBLs considered in this paper are HBLs with the exception of 4C 47.08 which is a LBL and all of the RBLs are LBLs with the exception of Mrk501 which is a HBL. In Section 4 comparison is made between the LBL and HBL samples with comment on the relation of these to the intermediate sample but because of the large overlap, the same general results apply to the RBL/XBL samples.

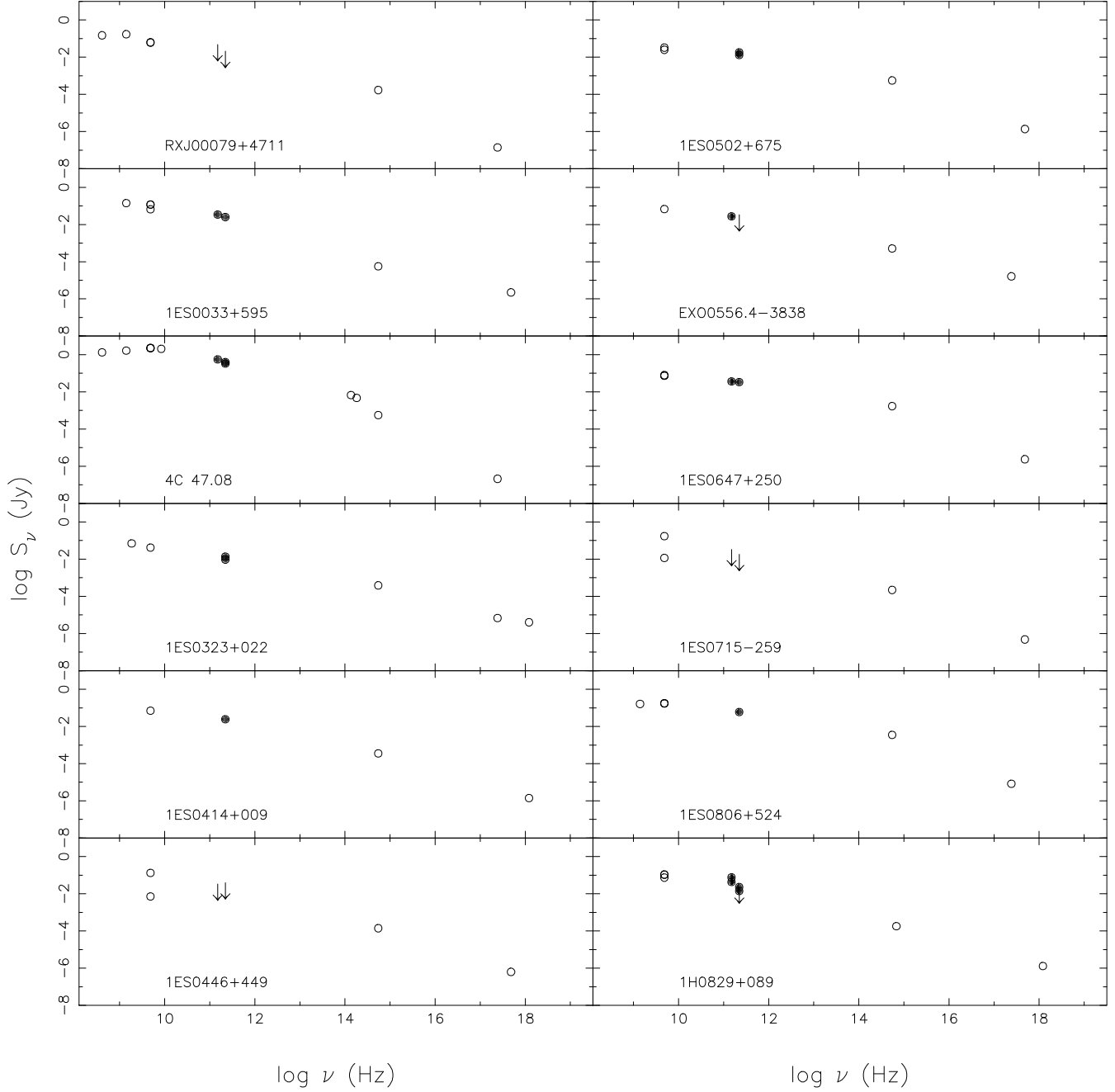
**Table 1.** Summary of the observations

source	UT date	2 mm (mJy)	1.35 mm (mJy)	0.85 mm (mJy)	$\alpha_5-230$	$\alpha_{230}-X$
(1)	(2)	(3)	(4)	(5)	(6)	(7)
RXJ 00079+4711	19970921	$3\sigma < 17.3$	...	...	...	...
	19970624	...	$3\sigma < 16.3$	...	$< -0.34$	$> -0.84$
	19980208	...	$3\sigma < 7.5$	...	$< -0.56$	$> -0.78$
	19980531	...	$3\sigma < 7.5$	...	$< -0.56$	$> -0.78$
1ES 0033+595 4C 47.08	19970921	$34.3 \pm 8.1$	$25.0 \pm 4.9$	...	-0.24	-0.64
	19980207	...	$328.6 \pm 46.8$	...	-0.50	-1.03
	19980531	$553.6 \pm 57.2$	$395.9 \pm 43.5$	...	-0.45	-1.04
1ES 0323+022	19980309	...	$13.6 \pm 2.9$	...	-0.29	-0.52
	19980531	...	$9.5 \pm 2.4$	...	-0.39	-0.52
1ES 0414+009	19980309	...	$24.2 \pm 3.6$	...	-0.28	-0.63
1ES 0446+449	19970815	$3\sigma < 12.1$	...	...	...	...
	19970921	...	$3\sigma < 14.3$	...	$< +0.18$	$> -0.69$
	19980310	...	$13.1 \pm 3.1$	...	-0.24	-0.63
1ES 0502+675	19980311	...	$18.2 \pm 3.3$	...	-0.15	-0.65
	19970921	$27.4 \pm 7.0$	...	...	...	...
	19980310	...	$3\sigma < 12.1$	...	$< -0.45$	$> -0.48$
1ES 0647+250	19970815	$36.3 \pm 8.5$	...	...	...	...
	19970921	...	$33.4 \pm 6.0$	...	-0.19	-0.65
	19970921	$3\sigma < 12.0$	$3\sigma < 6.5$	...	$< -0.15$	$> -0.65$
1ES 0806+524	19980310	...	$60.0 \pm 6.8$	...	-0.28	-0.64
1H 0829+089	19970921	$75.7 \pm 9.7$	$3\sigma < 8.4$	...	...	-0.57
	19980310	...	$14.1 \pm 2.5$	...	-0.52	-0.60
	19980424	$43.0 \pm 6.7$	$22.9 \pm 3.8$	...	-0.40	-0.63
1ES 1101-232	19980505	$16.1 \pm 5.2$	$14.9 \pm 4.2$	...	-0.39	-0.57
1ES 1212+078	19980505	$3\sigma < 27.4$	$17.7 \pm 3.6$	...	-0.44	-0.76
	19980706	...	$16.7 \pm 3.3$	...	-0.45	-0.76
	19980505	...	$12.6 \pm 4.0$	...	-0.31	-0.64
MS 1229.2+6430	19980706	...	$3\sigma < 11.8$	...	$< -0.33$	$> -0.64$
	19980505	$225.4 \pm 27.3$	$208.0 \pm 23.5$	...	-0.18	-0.92
RXJ 12302+2512	19980510	$3\sigma < 13.1$	$3\sigma < 12.3$	...	$< -0.39$	$> -0.58$
RXJ 16442+4546	19970702	$17.7 \pm 4.4$	$17.1 \pm 2.9$	...	-0.49	-0.79
4U 1722+11	19970605	$118.8 \pm 23.7$	...	...	...	...
	19980207	$204.9 \pm 21.3$	$188.2 \pm 19.3$	$182.8 \pm 21.0$	+0.18	-0.76
	19980207	$57.2 \pm 9.0$	$52.0 \pm 5.7$	...	-0.29	-0.74
EXO 1811.7+3143	19980207	$46.4 \pm 8.3$	$40.7 \pm 5.1$	...	-0.25	-0.94
1ES 1959+650	19970815	$144.0 \pm 19.3$	$149.0 \pm 24.8$	...	-0.14	-0.73
MS 2143.4+0704	19970815	$14.3 \pm 4.7$	$3\sigma < 21.8$	...	$< -0.22$	$> -0.79$
	19980208	...	$16.7 \pm 3.0$	...	-0.29	-0.77
	19980531	...	$11.8 \pm 2.5$	...	-0.38	-0.74
	19980607	$14.8 \pm 4.0$	...	...	...	...
1ES 2344+514	19970624	$78.9 \pm 11.0$	$54.1 \pm 10.4$	...	-0.36	-0.74
	19970815	$79.0 \pm 10.8$	...	...	...	...

### 3 OBSERVATIONS

The observations were made with the new submillimetre camera, SCUBA (Gear et al. 1998, in preparation; Holland et al. 1998,1999), on the 15-m James Clerk Maxwell Telescope (JCMT), Mauna Kea, Hawaii. SCUBA, operating at 75 mK, is optimised for mapping observations at submillimetre wavelengths but also has single bolometers operating at 2.0, 1.35 and 1.1 mm (the 1.1 mm detector was inoperable at the time of this work) corresponding approximately to 150, 230 and 270 GHz respectively. The NEFDs at 2.0 and 1.35 mm are typically measured as 120 and 60 mJyHz<sup>-1/2</sup> respectively (including chopping) and these values are largely insensitive to the atmospheric opacity. Photometric observations can also be made with the arrays, usually with the

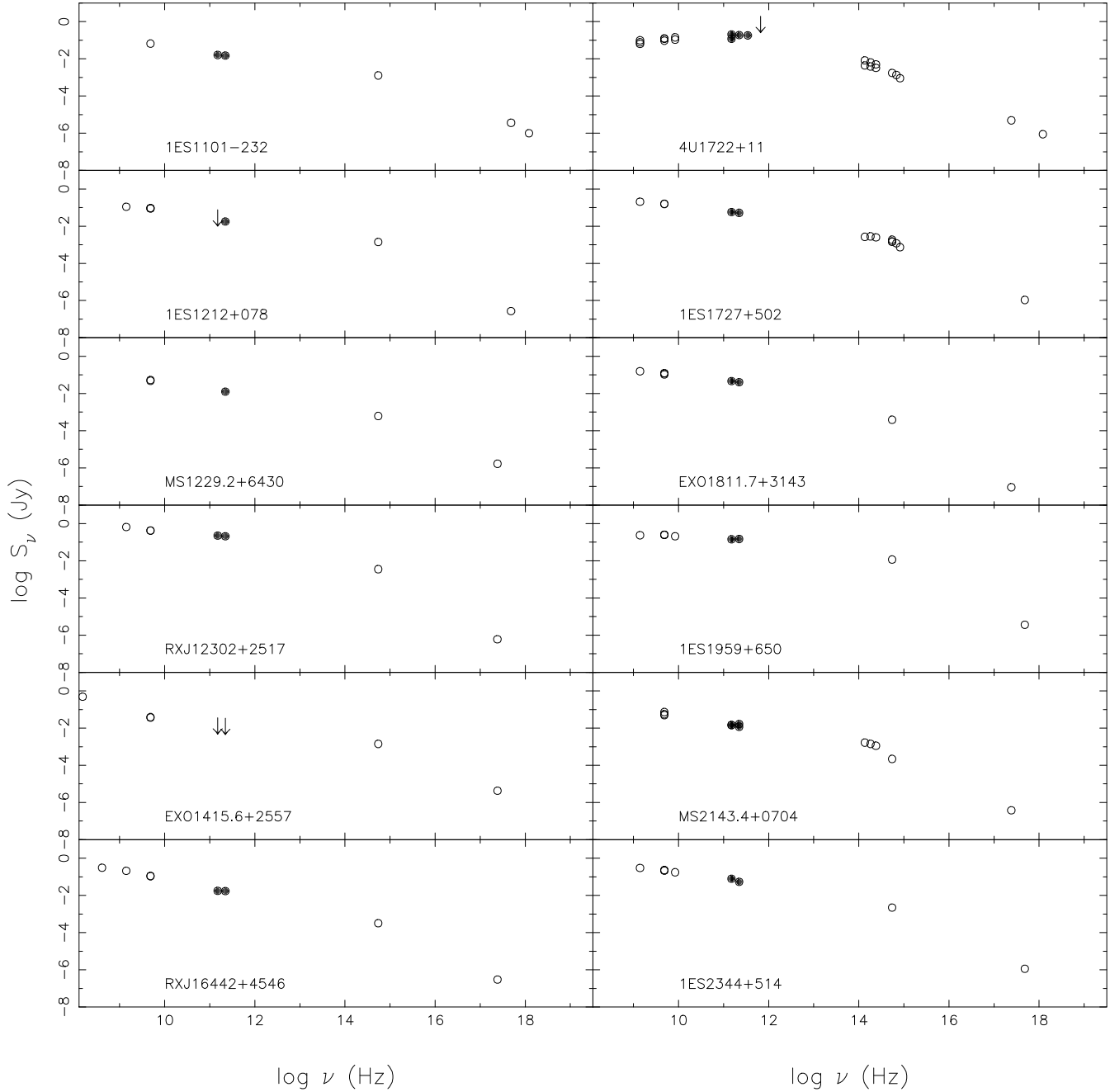
central pixel, and in this case the remaining bolometers can be used to subtract the sky emission which is correlated across the 2.3 arcmin field of view (Ivison et al. 1998; Jenness, Lightfoot & Holland 1998). Under average to poor conditions the NEFD at 0.85 mm (345 GHz) is  $\sim 90$ –200 mJyHz<sup>-1/2</sup>. The standard SCUBA photometry mode was used for the observations. A small square map consisting of nine pixels and centred on the source is made with an integration time of one second per pixel, the telescope then nods into the other beam where the procedure is repeated. The nine-point maps are then averaged to produce one photometric observation taking 18 seconds to complete. The pixel spacing was 3 arcsec at 2.0 and 1.35 mm and 2 arcsec at 0.85 mm and the chop throw was 60 arcsec at  $\sim 7.8$  Hz.



**Figure 2.** Broad-band spectra of the BL Lac objects. Millimetre data presented in this work are shown as filled symbols or upper limits.

The observations were typically made under relatively poor observing conditions, i.e. high levels of precipitable water vapour (pwv) and atmospheric refraction (sky noise). Thus almost all data were taken at 2.0 and 1.35 mm to optimise the sensitivity and reduce the effects of signal-loss due to sky noise and pointing errors (both giving variations of less than 3 arcsec whilst the beam sizes are in excess of 20 arcsec at these wavelengths). The atmospheric opacity was monitored regularly with skydips at both 0.85 mm using SCUBA and at 1.3 mm with the nearby Caltech Submillimeter Observatory (CSO) sky monitor. Standard relations

were used to convert these opacities to those relevant to the adopted SCUBA filters. The instrumental gain was measured on each night with observations of the planets Mars and/or Uranus. These gains are stable to within 10 per cent at 1.35 mm but may be elevation dependent at 2.0 mm with a total variation of order 20 per cent. We have assumed a calibration uncertainty of 10 per cent for all observations and these are added in quadrature with the uncertainty derived from the measured signal-to-noise ratio. Data reduction was performed with the standard SCUBA reduction

Figure 2. - *continued*

package and is analogous to that employed with previous instrumentation.

#### 4 RESULTS

The observational results are summarized in Table 1 where column (1) has the source name, (2) the UT date of the observation, (3), (4) and (5) the measured fluxes at 2.0, 1.35 and 0.85 mm, (6) the two-point spectral index,  $\alpha_{5-230}$  and (7) the two-point spectral index,  $\alpha_{230-X}$ . See below for the

definition of these quantities. Errors on the two-point spectral indices are not quoted since, because the data are non-simultaneous, it is impossible to quantify the effect of source variability.

Fig. 2 shows the broad band spectra of those objects listed in Table 1. These spectra were constructed with non-simultaneous data taken from the literature but because of the broad frequency range considered, variability will have only a marginal effect on the overall spectral shapes. The two radio galaxies mentioned in Section 2 are included in this figure and it should be noted that the radio spectra in-

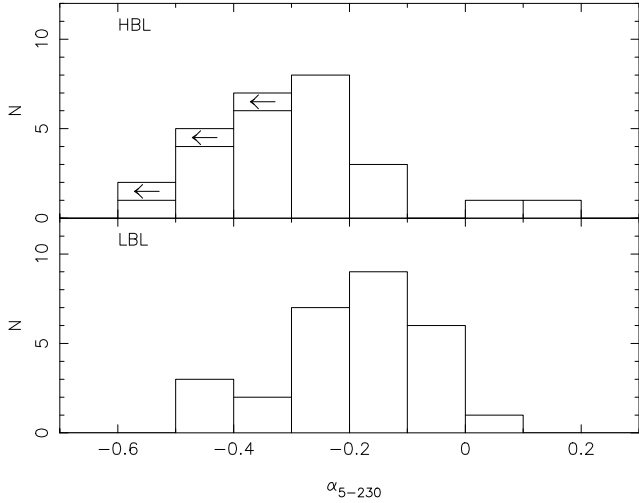


**Figure 3.** Histograms showing the 5 to 230 GHz spectral index ( $\alpha_{5-230}$ ) distribution for the HBLs (top) and LBLs (bottom).

clude fluxes for both the compact and extended emission, the latter providing the dominant contribution. Neither source was detected at millimetre wavelengths.

In general, the millimetre data fall close to a straight line connecting the 4.85 GHz point with the optical point and the millimetre flux is typically less than the radio flux as found for LBLs (Gear et al. 1994) and is thus likely to be optically thin unless the spectra have a complex structure.

Columns (6) and (7) of Table 1 list the two-point spectral indices between 5 GHz (or more strictly 4.85 GHz) and 230 GHz ( $\alpha_{5-230}$ ) and between 230 GHz and the X-ray band ( $\alpha_{230-X}$ ). The radio and X-ray data, which are not contemporaneous with the millimetre data, were taken from the literature (Padovani & Giommi 1995b and reference therein). These spectral index distributions for the HBL sample are shown in the upper panels of Figs. 3 and 4 where two sources detected previously at 230 GHz (Gear 1993b) are also included, namely MS 1402.3+0416 and MS 1534.2+0148 (both objects fulfill the HBL criterion defined in Section 2).

The lower panels of these figures show the corresponding distributions for the LBL sample. The radio and millimetre data used to calculate the LBL spectral indices (and the HBL Mrk 501) were taken from Gear et al. (1994) and are quasi-simultaneous (taken within  $\sim 4$  weeks) whilst the X-ray data (at 1 KeV) are from Urry et al. (1996) or, for 1514–241 and 2200+420 only, from Worrall & Wilkes (1990). Fig. 3 includes multiple epochs for individual sources since source variability can significantly affect the derived  $\alpha_{5-230}$  values even when the two fluxes are measured quasi-simultaneously (see Gear et al. 1994). In the case of non-detections, only the deepest upper limit is plotted. However, Fig. 4 only includes the first millimetre epoch of observation for each source taken from Gear et al. (1994) or Table 1. In this case, since variability will have little effect on  $\alpha_{230-X}$  due to the large separation in frequency space, inclusion of multiple epochs would bias the statistics.

The mean values of  $\alpha_{5-230}$  are  $-0.29 \pm 0.15$  for the HBLs and  $-0.19 \pm 0.14$  for the LBLs. A Kolmogorov-Smirnov (KS) test shows that the  $\alpha_{5-230}$  distributions are different at the

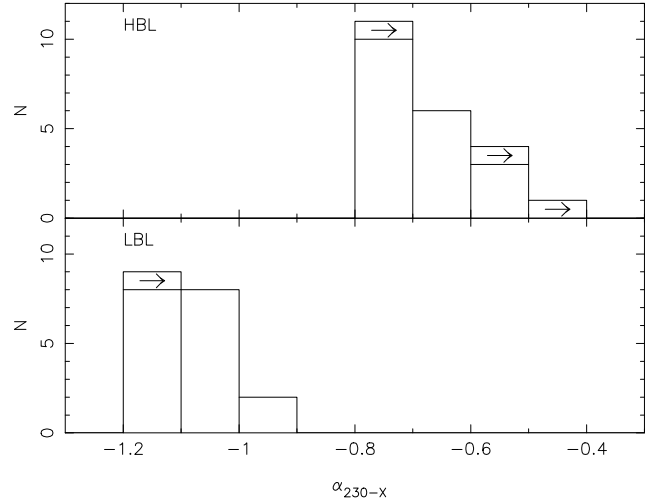


**Figure 4.** Histograms showing the 230 GHz to X-ray spectral index ( $\alpha_{230-X}$ ) distribution for the HBLs (top) and LBLs (bottom).

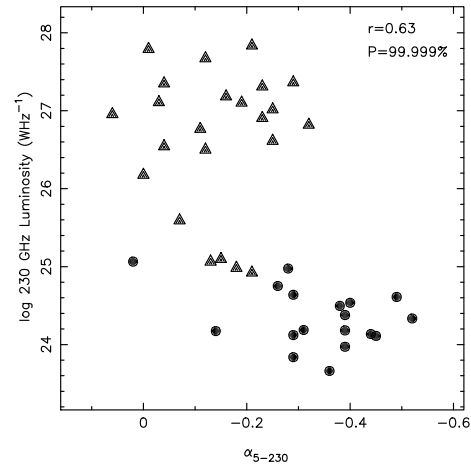


**Figure 5.** Correlation of  $\alpha_{5-230}$  with 230 GHz luminosity. Triangles are LBLs and circles are HBLs. The correlation coefficient,  $r$ , and its significance,  $P$ , are indicated on the plot.

99 per cent confidence level, or if the limits are assumed to be detections, 99.9 per cent confidence level, suggesting that the HBLs have slightly steeper spectra. Before concluding that this difference is an intrinsic property it is first necessary to investigate selection effects; for example, is  $\alpha_{5-230}$  correlated with either redshift or luminosity?

Fig. 5 shows that  $\alpha_{5-230}$  is indeed correlated with 230 GHz luminosity in the sense that more luminous objects have more positive values of  $\alpha_{5-230}$  (a Spearman rank-order correlation test gives  $r = 0.63$  at the  $P = > 99.99$  per cent confidence level) whereas Fig. 6 shows no strong correlation between  $\alpha_{5-230}$  and redshift ( $r = 0.32$ ,  $P = 95.6$  per cent). Subsequently, the correlation shown in Fig. 5 does not result from a correlation of luminosity with both redshift (not shown but expected for flux limited samples) and spectral index. Possible origins of this correlation are discussed in

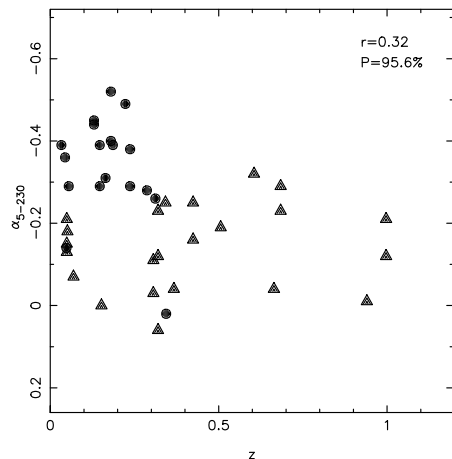


**Figure 6.** Correlation of  $\alpha_{5-230}$  with redshift. Triangles are LBLs and circles are HBLs. The correlation coefficient,  $r$ , and its significance,  $P$ , are indicated on the plot.

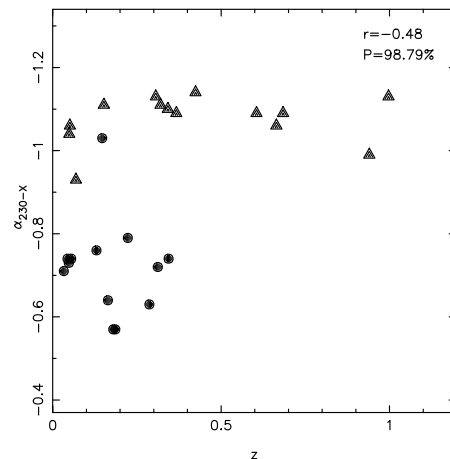


**Figure 8.** Correlation of  $\alpha_{230-X}$  with redshift. Triangles are LBLs and circles are HBLs. The correlation coefficient,  $r$ , and its significance,  $P$ , are indicated on the plot.

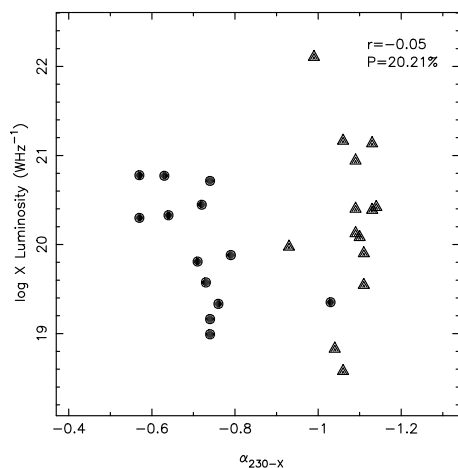


**Figure 7.** Correlation of  $\alpha_{230-X}$  with X-ray luminosity. Triangles are LBLs and circles are HBLs. The correlation coefficient,  $r$ , and its significance,  $P$ , are indicated on the plot.

the next section. It is thus found that *the radio-millimetre spectral indices of LBLs are slightly steeper than those of HBLs*.

The  $\alpha_{230-X}$  distributions (Fig. 4) are clearly different ( $>99.99$  per cent confidence with a KS test). Mean values of  $\alpha_{230-X}$  are  $-0.68 \pm 0.07$  for the HBLs and  $-1.08 \pm 0.06$  for the LBLs. An important point to note is that the two intermediate sources that were discussed in Section 2 have intermediate values of  $\alpha_{230-X}$  (both fall in the  $-0.9$  to  $-1.0$  bin; not shown). This point is discussed further in the next section.

Figs 7 and 8 show the correlations of  $\alpha_{230-X}$  with X-ray luminosity and redshift. Fig. 7 shows no correlation ( $r = -0.05$ ,  $P = 20.2$  per cent) whereas Fig. 8 shows a possible anti-correlation of spectral index with redshift ( $r = -0.48$ ,  $P = 98.85$  per cent) which is most likely an artefact caused by the different redshift distribution of LBLs and HBLs (e.g.

Gear et al. 1993b). It is concluded that *the millimetre to X-ray spectra of HBLs are significantly flatter than those of LBLs*.

## 5 DISCUSSION

The preceding analysis showed that there are probable differences between the  $\alpha_{5-230}$  distributions and distinct differences between the  $\alpha_{230-X}$  distributions of LBLs and HBLs. This section discusses whether these results are consistent with a beaming model in which the LBLs are aligned closer to the line-of-sight than the HBLs or whether intrinsic differences between the classes are required by the data.

### 5.1 The $\alpha_{5-230}$ distribution

In Section 4 it was found that the HBLs have slightly steeper spectra between 5 and 230 GHz than the LBLs and that this result might follow from the correlation of  $\alpha_{5-230}$  with 230 GHz luminosity. It is, however, possible that this correlation is spurious and results from comparing two groups of BL Lac objects with intrinsically different radio properties; note that Fig. 5 shows little overlap between the two classifications. This section investigates possible origins for the correlation assuming it is real.

One mechanism that can change both the luminosity and the spectrum is the relativistic Doppler effect, i.e. the beaming model. These models were first devised (Browne 1983) to link LBLs with an unbeamed parent population of Fanaroff-Riley class I radio galaxies (FRI; Fanaroff & Riley 1974). Subsequently, the HBLs, which display less extreme properties, were included in the same scheme but at larger viewing angles (less Doppler boosting) than the LBLs (Ghisellini & Maraschi 1989). Various studies suggest that the average angles to the line-of-sight are  $\sim 10^\circ$ ,  $20^\circ$  and  $60^\circ$  for the LBLs, HBLs and FRIs respectively (Urry, Padovani & Stickel 1991; Ghisellini et al. 1993; Kollgaard et al. 1996b).

The details of the correlation shown in Fig. 5 will depend on the location of the synchrotron self-absorption turn-over frequency with respect to the frequencies used to calculate the spectral index. More specifically, a correlation will only be observed if the turn-over is Doppler shifted through the observed frequency range.

The luminosity in the observer's frame,  $L_\nu$ , is related to that in the source frame (denoted  $'$ ) by  $L_\nu = \delta^q L'_\nu$  where  $\delta$  is the relativistic Doppler factor ( $\delta = [\Gamma_p - (\Gamma_p^2 - 1)^{1/2} \cos \theta]^{-1}$  where  $\Gamma_p$  is the pattern Lorentz factor and  $\theta$  is the viewing angle). The exponent  $q = 3 - \alpha$  for a spheroidal source whereas  $q = 2 - \alpha$  for a continuous jet. The former is assumed below but note that the continuous jet case requires a higher Doppler factor to produce a given luminosity. Using the same notation, the observed frequency  $\nu = \delta \nu'$ .

The intrinsic synchrotron spectrum of a BL Lac object can be represented by

$$L'_{\nu'} = C'(\nu'_1) \left( \frac{\nu'}{\nu'_1} \right)^\xi \left\{ 1 - \exp \left[ - \left( \frac{\nu'}{\nu'_1} \right)^{\alpha-\xi} \right] \right\} \quad (1)$$

where  $\alpha$  is the optically thin spectral index,  $\xi$  is the spectral index in the optically thick regime,  $\nu'_1$  is the frequency at which the optical depth equals unity and  $C'(\nu'_1)$  is a constant. It follows that

$$L_\nu = \delta^{3-\alpha} C'(\nu'_1) \left( \frac{\nu}{\delta \nu'_1} \right)^\xi \left\{ 1 - \exp \left[ - \left( \frac{\nu}{\delta \nu'_1} \right)^{\alpha-\xi} \right] \right\} \quad (2)$$

The intrinsic spectrum is constructed by assuming values for  $\alpha$ ,  $\xi$ ,  $\nu'_1$  and  $C'(\nu'_1)$ . Equation (2) can then be used to calculate the 230 and 5 GHz luminosities, and hence  $\alpha_{5-230}$ , in the observer's frame as a function of  $\delta$  (or  $\theta$  if a value for  $\Gamma_p$  is assumed). Fig. 9 shows several of these simple models plotted over the data shown in Fig. 5. The various parameters were chosen to give a good representation of the data and good agreement with the unified scheme, these being  $\alpha = -0.6$ ,  $\xi = 0.4$  and  $C'(\nu'_1) = 10^{25} \text{ WHz}^{-1}$ ; curves corresponding to values of  $\nu'_1 = 3, 8, 12, 16, 20$  GHz are plotted from right to left. Various values of  $\delta$  are shown on the solid curve ( $\nu'_1 = 8$  GHz). The corresponding values of  $\theta$  assume  $\Gamma_p = 5$  which is the approximate value indicated by both the measured superluminal speeds (Kollgaard et al. 1996b, and references therein) and luminosity function studies (Urry & Padovani 1995).

The model clearly provides a good representation of the observed correlation and is consistent with the unified scheme outlined above but are the assumed parameters reasonable? The optically thin spectral index,  $\alpha = -0.6$ , is close to that measured for large samples of radio sources (e.g. Conway, Kellerman & Long 1963) and thus appears a valid assumption. As  $\theta$  approaches  $90^\circ$  the measured value of  $\alpha_{5-230}$  will approach  $\alpha$  as indicated in Fig. 9 and so, for example, reducing  $\alpha$  will skew the envelope of models to the bottom right. Similarly increasing  $\xi$  will skew the envelope to the top left.

The value of  $\xi$  is difficult to constrain from existing observations. For a simple homogeneous source  $\xi = 2.5$  but the composite spectra of BL Lac objects are well known to be flatter than this in the radio regime. The data for LBLs (Gear et al. 1994) give  $\xi$  in the range 0.1–0.9 but values towards both ends of this distribution give poor representations of the observed correlation.

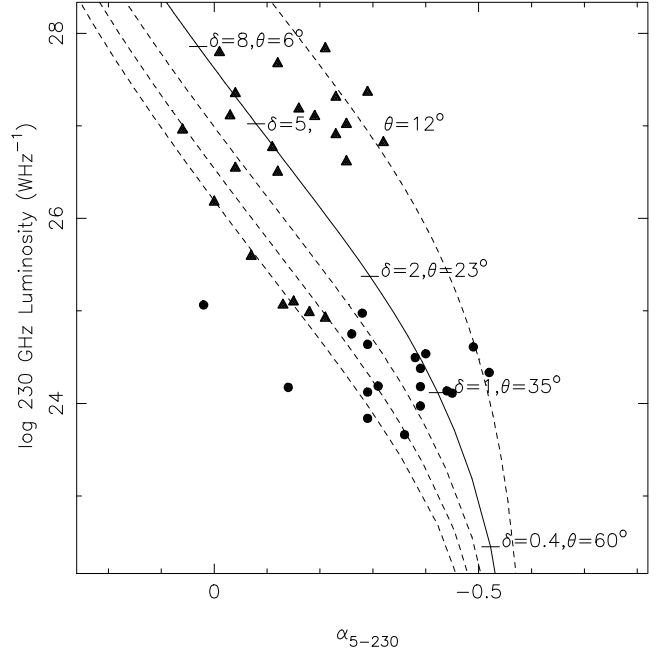


**Figure 9.** Simulated spectral index versus luminosity relationships plotted over the data shown in Fig. 5. The lines represent values of  $\nu'_1 = 3, 8, 12, 16, 20$  GHz (from right to left). Values of the relativistic Doppler factor, ( $\delta$ ) and viewing angle ( $\theta$  - see text) are shown on the solid curve for which  $\nu'_1 = 8$  GHz

The value of  $C'(\nu'_1)$  fixes the various values of  $\delta$  and  $\theta$  along the curves. Observations of FRI radio galaxies at 230 GHz would show whether the assumed value is reasonable but no data exist in the literature at this time. However, estimates of  $\delta$  for BL Lac objects (mostly LBLs) exist in the literature from both Synchrotron Self-Compton (SSC) models (e.g. Ghisellini et al. 1993) and variability studies (Teräsranta & Valtaoja 1994). The former study gives values of  $\delta = 0.01 - 14.3$  (mean =  $3.9 \pm 4.2$ ; 33 objects) with only four objects having  $\delta > 10$  whilst the latter gives  $\delta = 0.2 - 4.3$  (mean =  $1.4 \pm 1.2$ ; 11 objects). These values are roughly consistent with those derived above and support the choice of  $C'(\nu'_1)$ .

It is thus concluded that the correlation of  $\alpha_{5-230}$  with 230 GHz luminosity, if real, is consistent with that expected to arise if the LBLs and HBLs are Doppler boosted FRI radio galaxies. The parameters of the assumed model appear reasonable but are perhaps limited to a narrow range of acceptable values. However, it is important to note that such a simple model cannot be used to infer that all of the differences between the spectra of BL Lac objects can be explained within the framework of the beaming model. For example, Sambruna et al. (1996) showed that whilst the accelerating jet model (Ghisellini & Maraschi 1989) at a range of viewing angles can reproduce successfully some of the spectral differences between LBLs and HBLs, it does not lead to the observed wide range of peak frequency or  $\alpha_{\text{ro}}$ . These authors suggest that a difference in jet properties, such as magnetic field strength or jet size is required to explain the data. More recently, Fossati et al. (1997, 1998; see also Sam-

bruna et al. 1996) have suggested that a link exists between spectral shape and bolometric luminosity and this idea has been extended to unify BL Lac objects in terms of viewing angle and jet electron kinetic luminosity (Georganopoulos & Marscher 1998). For the latter model, the difference in luminosity between HBLs and LBLs is only partly attributed to a difference in viewing angle. Furthermore, it can explain the differences in redshift distribution and cosmological evolution between the two classes but, as noted by the authors, does not include a treatment of the inverse-Compton mechanism which may dominate the X-ray emission of LBLs (see next section).

## 5.2 The $\alpha_{230-X}$ distribution

The spectral index distributions between 230 GHz and the X-ray band are significantly different and tend to cluster around values of  $\sim -0.70$  for the HBLs and  $\sim -1.1$  for the LBLs although, as noted in Section 4, the two ‘intermediate’ BL Lac objects have intermediate values of  $\alpha_{230-X}$  ( $\sim -0.9$ ). More millimetre observations of BL Lac objects that fall in the intermediate region of the  $\alpha_{ox} - \alpha_{ro}$  diagram are needed to confirm this trend. The  $\alpha_{230-X}$  distributions show a more pronounced difference between the two classes than the  $\alpha_{rx}$  distributions. For example, Sambruna et al. (1996) find  $\alpha_{rx} = -0.57 \pm 0.06$  for the EMSS XBLs and  $\alpha_{rx} = -0.86 \pm 0.08$  for the ‘1 Jansky’ RBLs with some overlap between the two samples. This effect is likely to be due to the influence of synchrotron self-absorption on the radio fluxes whereas the 230 GHz emission is optically thin.

The clear dichotomy in  $\alpha_{230-X}$  certainly cannot be explained within the framework of the simple beaming model outlined in the previous section but conversely cannot be used as evidence that beaming is unimportant in these sources. As discussed above the beaming model in combination with one or more intrinsic differences between the two classes may provide the best fit to the data.

The data presented here as well as in the literature now strongly suggest that different mechanisms are responsible for the X-ray emission in the two classes. Padovani & Giommi (1996) have analysed the *ROSAT* X-ray spectra of a large sample of BL Lac objects. They find that the LBLs are characterised by concave optical–X-ray continua and have flatter X-ray spectra than the HBLs. The HBLs have convex overall broadband continua and the X-ray spectral slopes are well correlated with  $\alpha_{ox}$  and anti-correlated with the X-ray to radio flux and cutoff frequency. They conclude that the X-ray emission in HBLs is produced by the synchrotron process whereas that from LBLs emanates from the SSC mechanism. In this scenario the HBLs must have high-energy cutoffs to the synchrotron emission at higher frequencies (UV–X-ray) than do the LBLs (IR–optical) otherwise synchrotron emission would dominate in both cases.

The 230 GHz measurements presented here are on the high-frequency side of the self-absorption turn-over and provide a measure of the optically thin spectral index. The mean value of  $-0.68 \pm 0.07$  for the HBLs is strikingly similar to the canonical value for large samples of radio sources (e.g. Conway et al. 1963) providing strong evidence that the X-rays are produced by the synchrotron mechanism.

For the LBLs there is no *a priori* reason to assume that the observed spectral indices are not also produced by

the synchrotron process but with a different electron energy spectrum to the HBLs, although this situation appears somewhat contrived. A more realistic interpretation, taking into account the above discussion, is that the X-ray emission from the LBLs is inverse-Compton radiation. For the ‘intermediate’ sources it is natural to speculate that the X-ray emission comes from a combination of both mechanisms, requiring that the X-ray synchrotron emission is significantly steepened by radiative losses in these objects.

## 6 SUMMARY

Millimetre wavelength observations of 22 XBLs of which 19 are HBLs, 1 is a LBL and 2 are ‘intermediate’ sources have been used along with similar published data for LBLs to search for differences between the radio–millimetre–X-ray spectral energy distributions of these objects. We find:

(1) The  $\alpha_{5-230}$  two-point spectral indices of HBLs are slightly steeper than those of LBLs. Furthermore  $\alpha_{5-230}$  is correlated with 230 GHz luminosity. If this correlation is real, i.e. it is not a result of comparing two populations of BL Lac objects with intrinsically different radio properties, then it is consistent with existing unified schemes where BL Lac objects are FRI radio galaxies viewed along the jet axis, the HBLs being at larger viewing angles than the LBLs. The assumed parameters of this model, however, must take a relatively narrow range of values and it is unlikely that a difference in beaming parameters alone can unify LBLs, HBLs and FRIs.

(2) The  $\alpha_{230-X}$  two-point spectral indices of HBLs are significantly flatter than those of LBLs and have values consistent with those expected for synchrotron radiation. The X-ray emission from the LBLs is more likely to be produced by the inverse-Compton mechanism. Interestingly, the two ‘intermediate’ BL Lac objects also have intermediate values of  $\alpha_{230-X}$  suggesting that both processes contribute to the X-ray emission in these sources.

The analysis presented in this paper thus points to a unified model for BL Lac objects that combines a spread of viewing angles with a spread of intrinsic source parameters. In this respect the model of Georganopoulos & Marscher (1998), adapted to incorporate inverse-Compton losses appears promising.

## ACKNOWLEDGMENTS

The James Clerk Maxwell Telescope is operated by the Joint Astronomy Centre in Hilo, Hawaii on behalf of the parent organizations PPARC in the United Kingdom, the National Research Council of Canada and The Netherlands Organization for Scientific Research. This research has made use of the NASA/IPAC Extragalactic Database (NED) which is operated by the Jet Propulsion Laboratory, California Institute of Technology, under contract with the National Aeronautics and Space Administration. J.A.S. acknowledges the support of a PPARC PDRA.

## REFERENCES

- Bade N., Beckmann V., Douglas N. G., Barthel P. D., Engels D., Cordis L., Nass P., Voges W., 1998, *A&A*, 334, 459
- Blandford R. D., Rees M. J., 1978, in Wolfe A. N., ed., *Pittsburgh Conf. on BL Lac objects*. Pittsburgh Univ. Press, Pittsburgh, p. 328
- Browne I. W. A., 1983, *MNRAS*, 204, L23
- Conway R. G., Kellerman K. I., Long R. J., 1963, *MNRAS*, 125, 261
- Fanaroff B., Riley J. M., 1974, *MNRAS*, 167, 31P
- Fossati G., Celotti A., Ghisellini G., Maraschi L., 1997, *MNRAS*, 289, 136
- Fossati G., Maraschi L., Celotti A., Comastri A., Ghisellini G., 1998, *MNRAS*, in press
- Gear W. K., 1993a, *MNRAS*, 264, 919
- Gear W. K., 1993b, *MNRAS*, 264, L21
- Gear W. K., et al., 1994, *MNRAS*, 267, 167
- Georganopoulos M., Marscher A. P., 1998, *ApJ*, submitted (astro-ph/9806170)
- Ghisellini G., Maraschi L., 1989, *ApJ*, 340, 181
- Ghisellini G., Padovani P., Celotti A., Maraschi L., 1993, *ApJ*, 407, 65
- Giommi P., Padovani P., 1994, *MNRAS*, 268, L51
- Holland W. S., Cunningham C. R., Gear W. K., Jenness T., Laidlaw K., Lightfoot J. F., Robson E. I., 1998, in ed. T. Phillips, *Advanced Technology MMW, Radio and Terahertz Telescopes*, *Proc. SPIE* 3357, in press
- Holland W. S., et al., 1999, *MNRAS*, in press
- Iverson R. J. et al. 1998, *ApJ*, 494, 211
- Jannuzi B. T., Green R. F. French H., 1993a, *ApJ*, 404, 100
- Jannuzi B. T., Smith P. S., Elston R., 1993b, *ApJS*, 85, 265
- Jenness T., Lightfoot J. F., Holland W. S., 1998, in ed. T. Phillips, *Advanced Technology MMW, Radio and Terahertz Telescopes*, *Proc. SPIE* 3357, in press
- Kock A., Meisenheimer K., Brinkmann W., Neumann M., Siebert J., 1996, *A&A*, 307, 745
- Kollgaard R. I., Gabuzda D. C., Feigelson E. D., 1996a, *ApJ*, 460, 174
- Kollgaard R. I., Palma C., Laurent-Muehleisen S. A., Feigelson E. D., 1996b, *ApJ*, 465, 115
- Morris S. L., Stocke J. T., Gioia I. M., Schild R. E., Wolter A., Maccacaro T., Della Ceca R., 1991, *ApJ*, 380, 49
- Nass P., Bade N., Kollgaard R. I., Laurent-Muehleisen S. A., Reimers D., Voges W., 1996, 309, 419
- Padovani P., 1999, in *The BL Lac Phenomenon*, ed. L. Takalo, *ASP Conference Series*, in press (astro-ph/9901128)
- Padovani P., Giommi P., 1995a, *ApJ*, 444, 567
- Padovani P., Giommi P., 1995b, *MNRAS*, 277, 1477
- Padovani P., Giommi P., 1996, *MNRAS*, 279, 526
- Padovani P., Urry C. M., 1991, *ApJ*, 368, 373
- Perlman E. S., Stocke J. T., Wang Q. D., Morris S. L., 1996a, *ApJ*, 456, 451
- Perlman E. S., Stocke J. T., Schachter J. F., Elvis M., Ellingson E., Urry C. M., Potter M., Impey C. D., Kolchinsky P., 1996b, *ApJS*, 104, 251
- Perlman E. S., Padovani P., Giommi P., Sambruna R., Jones L. R., Tzioumis A., Reynolds J., 1998, *AJ*, 115, 1253
- Schwartz D. A., Brissenden R. J. V., Tuohy I. R., Feigelson E. D., Hertz P. L., Remillard R. A., 1989, in *BL Lac Objects*, eds L. Maraschi, T. Maccacaro and M.-H. Ulrich (Springer, Berlin), p. 209
- Stickel M., Padovani P., Urry C. M., Fried J. W., Kühr H., 1991, *ApJ*, 374, 431
- Sambruna R. M., Barr P., Giommi P., Maraschi L., Tagliaferri G., Treves A., 1994, *ApJ*, 434, 468
- Sambruna R. M., Maraschi L., Urry C. M., 1996, *ApJ*, 463, 444
- Stocke J. T., Morris S. L., Gioia I., Maccacaro T., Schild R. E., Wolter A., 1990, *ApJ*, 348, 141
- Teräsanta H., Valtaoja E., 1994, *A&A*, 283, 51
- Urry C. M., Padovani P., 1995, *PASP*, 107, 803
- Urry C. M., Padovani P., Stickel M., 1991, *ApJ*, 382, 501
- Urry C. M., Sambruna R. M., Worrall D. M., Kollgaard R. I., Feigelson E. D., Perlman E. D., Stocke J. T., 1996, *ApJ*, 463, 424
- Worrall D. M., Wilkes B. J., 1990, *ApJ*, 360, 396
- Wurtz R., 1994, Ph.D. thesis, Univ. Colorado, Boulder

This paper has been produced using the Royal Astronomical Society/Blackwell Science  $\text{\LaTeX}$  style file.